COMMUNICATION

Nanoscale stabilization of Li–sulfur batteries by atomic layer deposited Al$_2$O$_3$†

Xia Li,[a] Jian Liu,[a] Biqiong Wang,[ab] Mohammad N. Banis,[a] Biwei Xiao,[a] Ruying Li,[a] Tsun-Kong Sham[b] and Xueliang Sun*[a]

An atomic layer deposited (ALD) Al$_2$O$_3$ coating applied to sulfur cathodes has been studied in this paper. It is demonstrated that the Al$_2$O$_3$ coating improves the cycling stability of Li–sulfur batteries. The underlying mechanism by synchrotron-based X-ray photoelectron spectroscopy was investigated. The coating layer not only protects the polysulfide from dissolution, but also facilitates the utilization of sulfur, demonstrating improved electrochemical performances.

Li–sulfur batteries have been considered as one of the most promising power storage systems for electric vehicles, owing to their overwhelming advantages in specific capacity and energy density.[1–5] Moreover, sulfur is attractive in its low cost, abundance, and environmental benignity.[1–5] Nevertheless, the present Li–sulfur batteries suffer from two major problems, which seriously hinder their commercial application.[6–12] One major issue is the inherent insulating nature of sulfur and discharge products Li$_2$S$_n$ ($n < 2$), which greatly limits the performance of Li–sulfur batteries.[6–12] Another issue is that polysulfide species, the dissolved intermediate product, will migrate between two electrodes and chemically react with lithium metal or sulfur cathode directly, leading to a drastic corrosion of lithium metal and loss of sulfur active material. This phenomenon is known as "shuttle effect".[6–12]

To improve the conductivity of sulfur cathodes, the prevailing strategies are addition of carbon materials, which has been endeavoring to the prosperity of Li–S batteries.[6–14] On the other hand, it has been widely accepted that the "shuttle effect" could be alleviated by coating S-based composites with conductive polymer,[14,15] metal oxides,[16,17] as well as graphene and carbon papers,[13,18–21] et al. Atomic layer deposition (ALD) is a thin film

depositing technique which is featured with conformal growth, precisely controllable thickness, as well as fast and facile operating processes.[22–25] Recently, ALD has been exerted to coat the electrode materials in Li-ion batteries (LIBs), and proven to be effective to prevent unexpected side reactions and improve the performance of LIBs. However, the application of ALD coating Li–sulfur batteries has rarely been unveiled.[26–28] Yushin et al.[26] reported that Al$_2$O$_3$ coating by plasma-enhanced ALD could improve the cycling performance of Li–S batteries, owing to the suppressed deposition of Li$_2$S on electrodes by Al$_2$O$_3$ coating. Another research by Wang et al.[27] employed ALD-Al$_2$O$_3$ coated carbon paper as a reactivation layer between sulfur cathode and separator in cell, constructing a novel configuration for Li–sulfur batteries. However, detailed Al$_2$O$_3$ coating effects and reaction mechanisms have not been carried out.

Herein, the influence of Al$_2$O$_3$ coatings with different thicknesses by ALD on the performance of sulfur-based electrodes is studied in detail. It is found that 2-cycle Al$_2$O$_3$ coating ($\sim$0.2 nm in thickness) could effectively improve the performance of Li–S batteries. The underlying reason for the performance improvement was investigated by synchrotron-based X-ray photoelectron spectroscopy (XPS), and a working mechanism was proposed. It is found that AlF$_3$/LiAlO$_2$ ionic conductive layer is formed during cell operation derived from Al$_2$O$_3$ layer. The conformal ALD coating facilitates both the confinement of polysulfide and the high utilization of sulfur active material, leading to impressive electrochemical performance of Li–sulfur batteries.

In experimental part, commercial mesoporous carbon black (KJ EC600, US) was chosen as host of sulfur. The sulfur–carbon composites (C/S composite) were with 65 wt% sulfur load (see details in ESI† experimental part). To obtain Al$_2$O$_3$ coatings with different thicknesses, 2-, 5-, 10-, and 20-cycle Al$_2$O$_3$ by ALD were conducted directly on sulfur–carbon electrodes at 100 °C using TMA and H$_2$O as precursors (see details in ESI†). On the basis of ALD mechanism, the thickness of coating layer should increase linearly with stepwise ALD reactions. The thicknesses of 2-cycle and 20-cycle ALD coating are about 0.2 and 3 nm

[a]Department of Mechanical and Materials Engineering, University of Western Ontario, London, ON, N6A 5B9, Canada. E-mail: xsun@eng.uwo.ca; Fax: +1 519 661 3020; Tel: +1 519 661 2111 ext. 87759

[b]Department of Chemistry, University of Western Ontario, London, Ontario, N6A 5B7, Canada

Communication

theoretically.[22,29] The sulfur load of C/S composites after ALD processes got lower to 60 wt%, as shown in Fig. S1.†

Fig. 1 shows the field emission scanning electron microscopy (FE-SEM), and elemental mapping images of C/S composites with 2-cycle Al_2O_3 coating. Uniform aluminum elemental mapping of electrode is presented under micrometer magnitude, indicating the conformal Al_2O_3 ALD coating growth on the surface of electrode. Typical morphologies and Al elemental mapping images of 5, 10, and 20-cycle are shown in Fig. S2.† The typical morphologies of these four samples with Al_2O_3 coating are agglomerated nanoparticles within a size of 30–40 nm, comparable with bare C/S electrode (Fig. S3†).

Electrochemical performances of C/S electrodes with and without Al_2O_3 coating are illustrated in Fig. 2. It is well known that the peak position and area of CV profiles are contingent on the conductivity of electrodes, the utilization of active materials, and the reversibility of batteries.[30,31] As shown in Fig. 2a, all the electrodes present two cathodic peaks at 2.3 V and 2.1 V, and one anodic peak at 2.4 V, both of which are consistent with regular Li–sulfur CV profiles. Interestingly, compared with bare C/S electrode, 2-cycle and 5-cycle Al_2O_3 coated electrodes exhibit lower intensity of anodic peaks, but comparable intensity of cathodic peaks. This phenomenon strongly suggests that ultrathin Al_2O_3 coating relieves the "shuttle effect" with the conductivity of coated electrodes preserved. On the other hand, in CV profiles, the normalized sweeping areas of 10-cycle and 20-cycle Al_2O_3 electrodes are much smaller than those of other samples. The reason is that the thicker Al_2O_3 layers block the Li-ion diffusion, leading to reduced sulfur utilization in cell operation.

Cycling performances of the electrodes with and without Al_2O_3 coatings under 0.1 C (160 mA g^{-1}) are presented in Fig. 2b. The pristine C/S composites show an unstable cycling performance with very low coulombic efficiency (stabilized at 70%). After 70 cycles, the discharge capacity only remains 460 mA h g^{-1}. In contrast, the 2-cycle Al_2O_3 coated C/S cathode
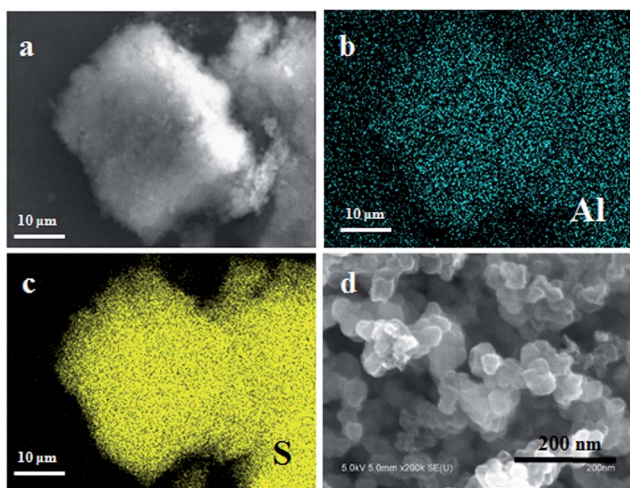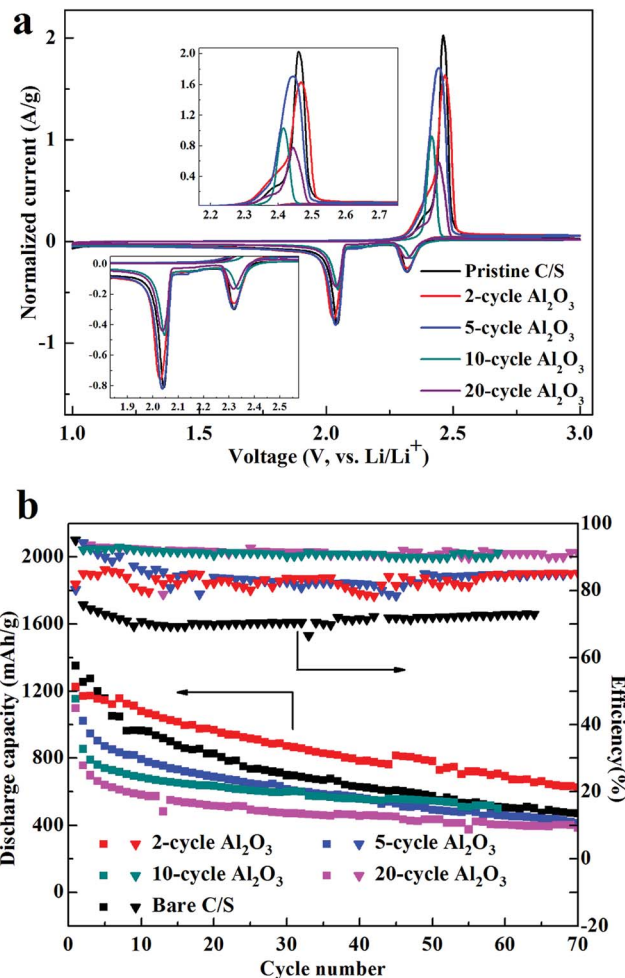

Fig. 2 (a) Typical cyclic voltammograms and (b) cycle performance of sulfur cathodes with and without Al_2O_3 coating.

exhibits an improved cycling performance. The battery during initial 20 cycles is more stable than that of the bare one. After 70 cycles, the discharge capacity keeps 640 mA h g^{-1}, indicating that the ultrathin Al_2O_3 coating can significantly improve the performance of sulfur cathode. On the other hand, cycling performances of 10-cycle and 20-cycle Al_2O_3 are not as good as 2-cycle. Although 20-cycle Al_2O_3 electrode displays an enhanced cycling stability, the first and 10th cycle discharge capacities are only about 1099 and 590 mA h g^{-1}, corresponding to limited sulfur utilization, well consisted with CV profiles.

Interestingly, the C/S cathodes deliver gradually elevated coulombic efficiencies with increasing Al_2O_3 coating cycles. Especially, the electrodes with 10-cycle and 20-cycle Al_2O_3 coating display coulombic efficiencies over 90%, in comparison with 70% of bare C/S composite. The improved coulombic efficiency indicates that Al_2O_3 coating can relieve the "shuttle effect". FE-SEM images of electrodes after 30 discharge–charge cycles further reveal the protection of polysulfides by Al_2O_3 coating. The Al_2O_3 coated electrodes show fewer discharge products deposited onto the surface (Fig. 3b and c), while the bare C/S electrode is almost totally covered by bulk of discharge products (Fig. 3a). Based on aforementioned discussion, Al_2O_3
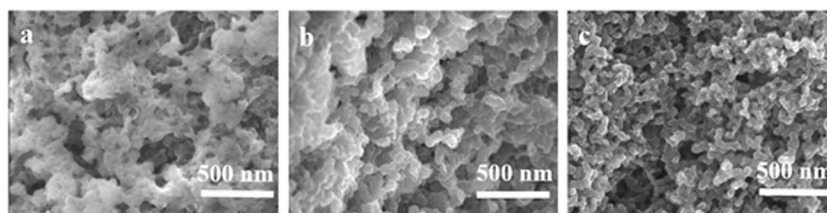

Fig. 1 (a–c) FE-SEM, elemental mapping images and (d) FE-SEM image under high magnification of C/S composites with 2-cycle Al_2O_3 coating.

Fig. 3 FE-SEM images of (a) pristine carbon–sulfur electrode, (b) 5-cycle, and (c) 20-cycle Al_2O_3 coated electrodes after 30 discharge–charge cycles.

coating is responsible for the restrained polysulfide dissolution and the suppression of insulated discharge product deposition. With ultrathin coating (2-cycle Al_2O_3), sulfur cathode performs much better cycling capacities and stability. Thicker ALD coating (10-cycle, 20-cycle Al_2O_3) delivers higher stability but reduced cycling capacities for sulfur cathodes. It should be mentioned that although Al_2O_3 coating can relieve the dissolution of polysulfide, it still cannot totally eliminate the "shuttle effect" since Al_2O_3 is a brittle material with limited durability.

Synchrotron-based XPS was carried out in order to elucidate the reason for the improved performance with ultrathin Al_2O_3 coating. Al 2p XPS spectra are shown in Fig. 4a. The intensities of Al 2p peaks are gradually strengthened from 2-cycle to 10-cycle Al_2O_3 coating, demonstrating a thicker coating layer formation with increasing ALD cycles. Moreover, Al 2p peaks of electrodes with increasing Al_2O_3 layers are distributed from high to low binding energy after battery test. Two major Al 2p peaks display in all of the spectra, as shown in Fig. 4b, one at 75.5 eV assigned to Al_2O_3, and the other at 77.5 eV to AlF_3.[32] Al 2p peaks of 2-cycle Al_2O_3 electrode, except for AlF_3 and Al_2O_3, another weak peak at about 72.2 eV is also observed which can be assigned to $LiAlO_2$.[32,33] It has been reported by Xiao's group that the formation of AlF_3 and $LiAlO_2$ is favorable to the ionic conductivity of cells, which reduces the energy barriers of Li-ion
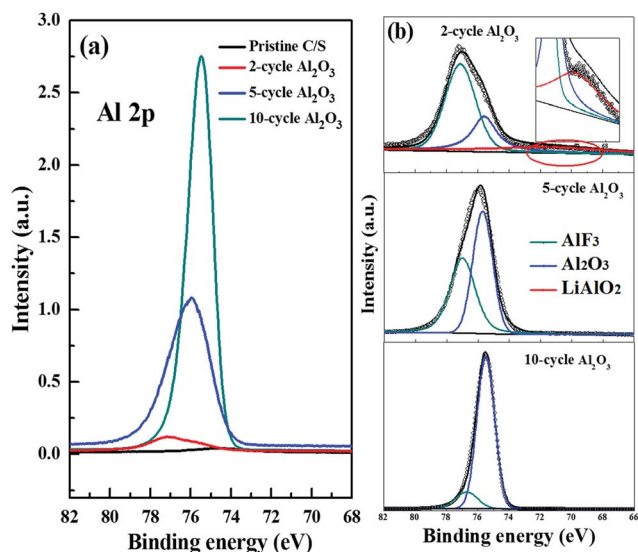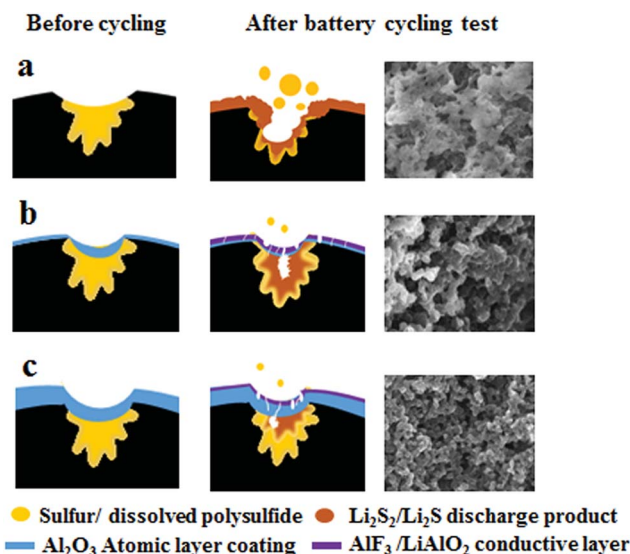

Fig. 5 Proposed mechanism of Al_2O_3 coating effects on sulfur cathodes with (a) blank, (b) ultrathin, and (c) relatively thick Al_2O_3 coating.

diffusion.[32] Thus, in our case, an artificial ionic conductive SEI layer is formed from the Al_2O_3 coating after lithiation/delithiation processes. The ionic conductive SEI layer is not only a protection of polysulfide, but also a support for Li-ion diffusion, resulting in high utilization and reversibility of sulfur cathode (shown in Fig. 5b).[29] Al 2p spectrum of 10-cycle Al_2O_3 electrode also shows two peaks of AlF_3 and Al_2O_3. However, it exhibits a strong peak of Al_2O_3 and a weak one of AlF_3, suggesting that the formation of AlF_3 and $LiAlO_2$ only occurred on the top layer of ALD coating. Despite the effective protection on polysulfides, thicker Al_2O_3 coating reduces the utilization of sulfur due to the insulating coating layer, resulting in a high cycling stability with lower capacities (shown in Fig. 5c).

Conclusions

In this paper, we studied a series of ALD Al_2O_3 coating on the performance of carbon–sulfur electrodes. The 2-cycle ALD Al_2O_3 electrode showed an impressive cycling capacity compared with bare C/S electrode, of which the discharge capacity maintained 630 mA h g^{-1} after 70 cycles. 10-cycle and 20-cycle ALD Al_2O_3 electrodes achieved coulombic efficiency over 90%, demonstrating a significant improvement of battery cycling stability. Confirmed by synchrotron-based XPS result, AlF_3/$LiAlO_2$ layer

Fig. 4 Synchrotron based Al 2p XPS spectra of (a) electrodes after cycling and (b) deconvolution of each spectrum.

was formed during lithiation/delithiation processes which served as an ionic conductive layer to improve the utilization of sulfur active material. Thereby, ALD Al_2O_3 coating performs as an SEI layer to preserve polysulfides migration and suppress the deposition of insulating discharge product on electrodes, improving both the stability and capacities of Li–S batteries. This work elucidates ALD Al_2O_3 coating effects on sulfur cathodes and will inspire advanced ALD applications on Li–sulfur batteries.

Acknowledgements

References

1 P. G. Bruce, S. A. Freunberger, L. J. Hardwick and J. M. Tarascon, *Nat. Mater.*, 2012, **11**, 19–29.

2 S. Evers and L. F. Nazar, *Acc. Chem. Res.*, 2013, **46**, 1135–1143.

3 X.-P. Gao and H.-X. Yang, *Energy Environ Sci*, 2010, **3**, 174.

4 A. Manthiram, Y. Fu and Y. S. Su, *Acc. Chem. Res.*, 2013, **46**, 1124–1134.

5 M. K. Song, E. J. Cairns and Y. Zhang, *Nanoscale*, 2013, **5**, 2186–2204.

6 S. H. Chung and A. Manthiram, *Adv. Mater.*, 2014, **26**, 1360–1365.

7 G. He, S. Evers, X. Liang, M. Cuisinier, A. Garsuch and L. F. Nazar, *ACS Nano*, 2013, **7**, 10920–10930.

8 X. Ji, K. T. Lee and L. F. Nazar, *Nat. Mater.*, 2009, **8**, 500–506.

9 S. Moon, Y. H. Jung, W. K. Jung, D. S. Jung, J. W. Choi and K. Kim do, *Adv. Mater.*, 2013, **25**, 6547–6553.

10 Y. X. Yin, S. Xin, Y. G. Guo and L. J. Wan, *Angew. Chem., Int. Ed. Engl.*, 2013, **52**, 13186–13200.

11 B. Zhang, X. Qin, G. R. Li and X. P. Gao, *Energy Environ. Sci.*, 2010, **3**, 1531.

12 C. Zhao, L. Liu, H. Zhao, A. Krall, Z. Wen, J. Chen, P. Hurley, J. Jiang and Y. Li, *Nanoscale*, 2013, **6**, 882–888.

13 R. Chen, T. Zhao, J. Lu, F. Wu, L. Li, J. Chen, G. Tan, Y. Ye and K. Amine, *Nano Lett.*, 2013, **13**, 4642–4649.

14 W. Li, Q. Zhang, G. Zheng, Z. W. Seh, H. Yao and Y. Cui, *Nano Lett.*, 2013, **13**, 5534–5540.

15 L. Wang, Z. Dong, D. Wang, F. Zhang and J. Jin, *Nano Lett.*, 2013, **13**, 6244–6250.

16 Z. Wei Seh, W. Li, J. J. Cha, G. Zheng, Y. Yang, M. T. McDowell, P. C. Hsu and Y. Cui, *Nat. Commun.*, 2013, **4**, 1331.

17 K. T. Lee, R. Black, T. Yim, X. Ji and L. F. Nazar, *Adv. Energy Mater.*, 2012, **2**, 1490–1496.

18 S. Evers and L. F. Nazar, *Chem. Commun.*, 2012, **48**, 1233–1235.

19 H. Wang, Y. Yang, Y. Liang, J. T. Robinson, Y. Li, A. Jackson, Y. Cui and H. Dai, *Nano Lett.*, 2011, **11**, 2644–2647.

20 J. Rong, M. Ge, X. Fang and C. Zhou, *Nano Lett.*, 2014, **14**, 473–479.

21 Y. S. Su and A. Manthiram, *Nat. Commun.*, 2012, **3**, 1166.

22 X. Li, J. Liu, M. N. Banis, A. Lushington, R. Li, M. Cai and X. Sun, *Energy Environ. Sci.*, 2014, **7**, 768.

23 X. Li, J. Liu, X. Meng, Y. Tang, M. N. Banis, J. Yang, Y. Hu, R. Li, M. Cai and X. Sun, *J. Power Sources*, 2014, **247**, 57–69.

24 J. Liu, X. Li, M. Cai, R. Li and X. Sun, *Electrochim. Acta*, 2013, **93**, 195–201.

25 X. Meng, X. Q. Yang and X. Sun, *Adv. Mater.*, 2012, **24**, 3589–3615.

26 H. Kim, J. T. Lee, D.-C. Lee, A. Magasinski, W.-i. Cho and G. Yushin, *Adv. Energy Mater.*, 2013, **3**, 1308–1315.

27 X. Han, Y. Xu, X. Chen, Y.-C. Chen, N. Weadock, J. Wan, H. Zhu, Y. Liu, H. Li, G. Rubloff, C. Wang and L. Hu, *Nano Energy*, 2013, **2**, 1197–1206.

28 M. Yu, W. Yuan, C. Li, J.-D. Hong and G. Shi, *J. Mater. Chem. A*, 2014, **2**, 7360–7366.

29 D. Wang, J. Yang, J. Liu, X. Li, R. Li, M. Cai, T.-K. Sham and X. Sun, *J. Mater. Chem. A*, 2014, **2**, 2306.

30 X. Li, Y. Hu, J. Liu, A. Lushington, R. Li and X. Sun, *Nanoscale*, 2013, **5**, 12607–12615.

31 J. Yang, J. Wang, Y. Tang, D. Wang, X. Li, Y. Hu, R. Li, G. Liang, T.-K. Sham and X. Sun, *Energy Environ. Sci.*, 2013, **6**, 1521.

32 X. Xiao, P. Lu and D. Ahn, *Adv. Mater.*, 2011, **23**, 3911–3915.

33 Y. He, X. Yu, Y. Wang, H. Li and X. Huang, *Adv. Mater.*, 2011, **23**, 4938–4941.